

Multiferroic nanoregions and a memory effect in cupric oxide

W. B. Wu,¹ D. J. Huang,^{1,2,*} J. Okamoto,¹ S. W. Huang,^{3,1} Y. Sekio,⁴ T. Kimura,⁴ and C. T. Chen¹

¹National Synchrotron Radiation Research Center, Hsinchu 30076, Taiwan

²Department of Physics, National Tsing Hua University, Hsinchu 30013, Taiwan

³Department of Electrophysics, National Chiao-Tung University, Hsinchu 30010, Taiwan

⁴Division of Materials Physics, Graduate School of Engineering and Science, Osaka University, Osaka 560-8531, Japan

(Received 11 March 2010; published 24 May 2010)

We report the observation of multiferroic nanoregions in cupric oxide, CuO, by means of resonant soft x-ray magnetic scattering. There exists an anomalous memory effect for the direction of the electric polarization in the commensurate-incommensurate magnetic transition that coincides with the ferroelectric transition. Scattering results, incorporated with simulations of diffuse scattering, lead us to propose a scenario that preserved spin handedness in the multiferroic nanoregions is responsible for this memory effect in the magnetically induced ferroelectric properties of CuO.

DOI: [10.1103/PhysRevB.81.172409](https://doi.org/10.1103/PhysRevB.81.172409)

PACS number(s): 75.25.-j, 71.30.+h, 78.70.Ck

Transition-metal oxides exhibit various intriguing phenomena such as high-temperature superconductivity and colossal magnetoresistance.¹ Recent extensive studies unveil another potential of transition-metal oxides as multiferroics in which magnetism and ferroelectricity coexist and are coupled.^{2–7} Efforts to understand their mechanisms reveal that the local inhomogeneity of the electronic structure often plays a crucial role in such properties.⁸ One well-known issue is the formation of local ferroelectric (FE) clusters embedded in a paraelectric (PE) matrix, known as “polar nanoregions,” which govern exceptional dielectric properties of “relaxors”—ferroelectrics in a special class with giant piezoelectric effects.⁹ In analogy to polar nanoregions in relaxors, “multiferroic nanoregions” are expected to form in some multiferroics and to prescribe their magnetoelectric properties.

The magnetoelectric coupling of many spiral magnets is explicable in terms of antisymmetric spin interactions.^{10,11} A breakdown of the inversion symmetry of the magnetism allows ferroelectricity, but the magnetism of such magnets typically occurs at temperatures that are too low to be practically useful. The magnetically induced ferroelectricity of most multiferroics tends to exist only at temperatures lower than ~ 40 K. Recently, Kimura *et al.*¹² discovered that cuprate CuO exhibits multiferroicity at temperatures below 230 K. This finding indicates that spiral magnetic order of a low-dimensional cuprate and a magnetically induced ferroelectric state at high temperatures can be simultaneously stabilized, yielding multiferroics in a new class with significantly high-ordering temperatures.

The monoclinic crystal structure of CuO comprises zigzag Cu-O chains of two types running along the $[10\bar{1}]$ and $[101]$ directions, as depicted in Fig. 1(a). The Cu-O-Cu bond angle ϕ is 146° in the $[10\bar{1}]$ chains and 109° in the $[101]$ chains; the former gives rise to a dominant superexchange interaction $J=60\text{--}80$ meV.^{13,14} CuO undergoes two successive magnetic transitions at $T_{N1}=213$ K and $T_{N2}=230$ K.^{13,15} At temperatures below T_{N1} , the magnetic moments are aligned collinearly along the b axis and order antiferromagnetically along the $[10\bar{1}]$ chains and ferromagnetically along the $[101]$ chains. In such a phase, the spin ordering is commensurate

(CM) with the lattice structure; the modulation vector is $(\frac{1}{2}, 0, -\frac{1}{2})$ in reciprocal lattice units. In contrast to the collinear spin structure, because of the competing ferromagnetic and antiferromagnetic interactions, CuO exhibits an incommensurate (ICM) spiral magnetic structure^{16,17} for only temperatures between T_{N1} and T_{N2} . The electric polarization (P) of CuO is thus induced by spin spirals through the antisymmetric superexchange interaction involving spin-orbit coupling.^{10,11}

We observed an anomalous memory effect for the direction of P in the CM-ICM magnetic transition that coincides with the ferroelectric transition. Figure 1(b) displays temperature (T) profiles of P along the b axis in a CuO single crystal. The electric polarization was obtained from integration of the pyroelectric current by time. We show in Fig. 1(b) two sets of P - T data in terms of different poling procedures. For the P - T data labeled as “Proper \pm poling,” in Fig. 1(b), we performed a proper poling procedure in which the poling electric fields ($E_{\text{pole}} = \pm 117$ kV/m) were applied above T_{N2} and then removed at a temperature (220 K) between T_{N1} and T_{N2} .¹² After the poling procedure, the measurements were done during temperature up (light-colored lines) and down (dark-colored lines) sweeps. The results, i.e., the absence of P below T_{N1} and above T_{N2} , and the sign change in P by changing that of E_{pole} , confirmed that the system shows ferroelectricity only in the ICM spiral phase. For the P - T data labeled as “memory effect,” in Fig. 1(b), the crystal was poled differently. We first cooled the crystal from above T_{N2} , while applying E_{pole} , and then removed the poling electric field at a temperature well below T_{N1} . The pyroelectric current was measured while heating the sample. If the phase below T_{N1} were truly paraelectric, the crystal would not memorize the polarity of the poling electric field after this poling procedure. However, as shown in Fig. 1(b), the crystal retains its original polarity of the poling electric field or the electric polarization at the ICM phase, i.e., there is a memory effect, although no substantial electric polarization exists below T_{N1} . In addition, the magnitude of the obtained P is almost equivalent to that obtained with the proper poling procedure (purple and green lines). Note that substantial electric polarization and memory effect were observed only

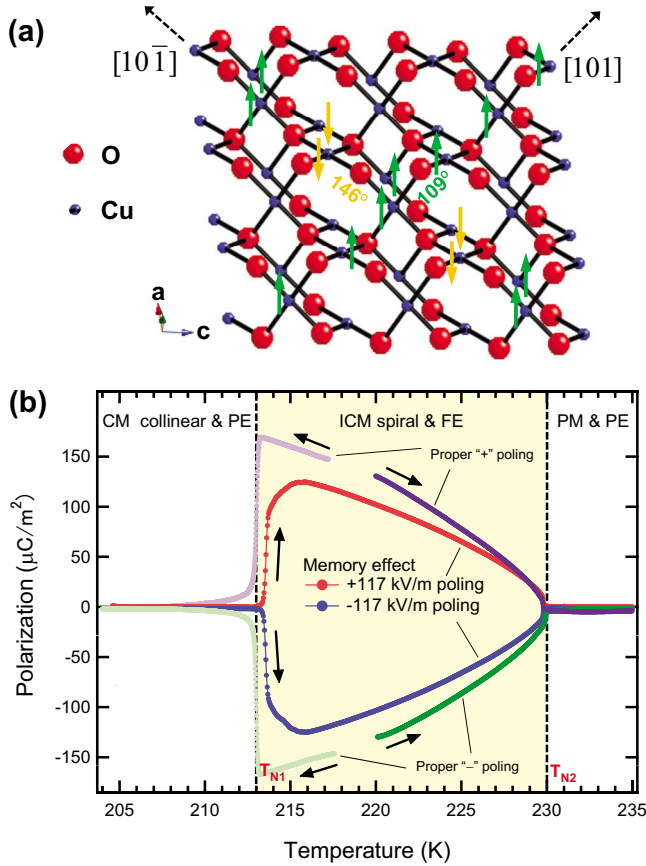


FIG. 1. (Color online) Zigzag Cu-O chains and memory effect of a CuO crystal. (a) Illustration of zigzag Cu-O chains of two types running along $[10\bar{1}]$ and $[101]$ with a collinear CM antiferromagnetic structure. Thick arrows indicate the spin directions of Cu^{2+} . The Cu-O-Cu bond angles along the $[10\bar{1}]$ and $[101]$ chains are 146° and 109° , respectively. (b) Temperature profiles of electric polarization along the b axis. The measurements were done at zero electric fields after cooling the crystal with $E_{\text{pole}} = \pm 117$ kV/m down to $T < T_{N1}$ (red and blue lines) and $T_{N1} < T < T_{N2}$ (purple and green lines). PM, PE, and FE denote paramagnetic, paraelectric, and ferroelectric, respectively.

along the b axis. Such anisotropic behavior cannot be explained in terms of thermally stimulated depolarization current.¹⁸ Similar anomalous memory effects have been observed at multiferroic transitions in other multiferroic spiral magnets such as TbMnO_3 (Ref. 19) and MnWO_4 .^{20,21} Although, based on measurements of bulk properties in the former studies, several origins for the memory effects have been proposed (e.g., the existence of additional domain walls, polar nuclei, or ferroelectric embryos, etc.), no microscopic experimental evidence has been provided so far.

To understand the observed memory effect in the multiferroic transition, we resorted to soft x-ray magnetic scattering.²² In the resonant L -edge x-ray scattering involved with a dipole-allowed $2p \rightarrow 3d$ transition, the magnetic scattering amplitude that depends linearly on the direction of the magnetic moment \mathbf{Z} is written as²³

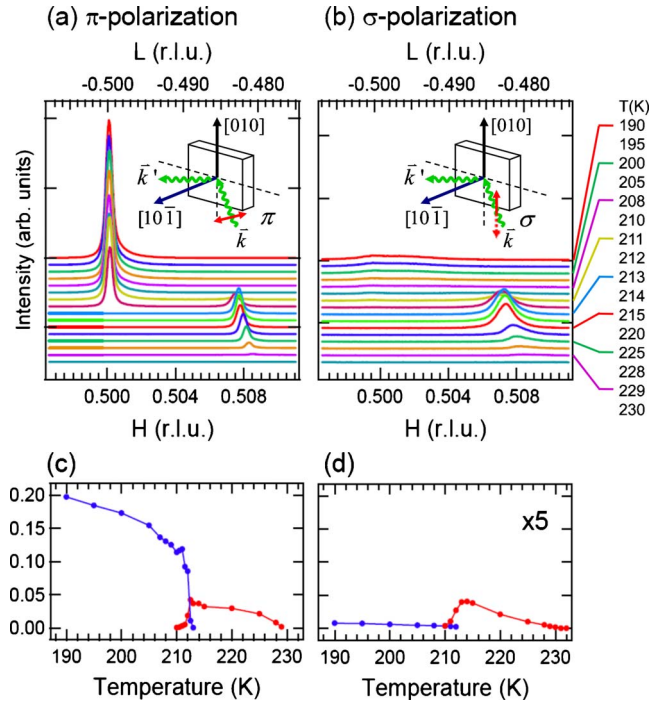


FIG. 2. (Color online) Temperature-dependent resonant soft x-ray magnetic scattering of CuO. (a) and (b) Momentum-transfer scans with π and σ polarizations at various temperatures as $\mathbf{q} = (H, 0, L)$ sweeps in the direction oriented along the modulation vector \mathbf{Q} . (c) and (d) Scattering intensity vs temperature with π and σ polarizations, respectively. Blue (red) circles are peak heights of the corresponding q scans depicted in (a) and (b) for the CM (ICM) phase; solid lines are guides for the eye.

$$f_{\text{res}}^{\text{mag}} = -i \frac{3\lambda}{8\pi} (\boldsymbol{\epsilon}_2^* \times \boldsymbol{\epsilon}_1) \cdot \hat{\mathbf{Z}} [F_{1,1} - F_{1,-1}], \quad (1)$$

in which $\boldsymbol{\epsilon}_1$ and $\boldsymbol{\epsilon}_2$ are the electric field vectors of incident and scattered x rays, respectively, and λ is the wavelength of x rays. $F_{1,1}$ and $F_{1,-1}$ are the scattering amplitudes corresponding to transitions with changes in the magnetic quantum number being 1 and -1 , respectively. For $\boldsymbol{\epsilon}_1$ perpendicular to the scattering plane, i.e., σ polarization, resonant x-ray magnetic scattering is sensitive only to spin in the scattering plane, whereas the scattering with $\boldsymbol{\epsilon}_1$ lying in the scattering plane (π polarization) is sensitive to spin perpendicular to or in the scattering plane, dependent on the direction of $\boldsymbol{\epsilon}_2$.

We measured resonant soft x-ray magnetic scattering on CuO single crystals with the EPU beamline of National Synchrotron Radiation Research Center (NSRRC), Taiwan. The momentum transfer \mathbf{q} between incident and scattered x rays lies in the a^*c^* plane, i.e., $\mathbf{q} = (q_a, 0, q_c)$. To reduce self-absorption, the photon energy was set to 923.5 eV, an energy just below the Cu L_3 -edge absorption. We found that magnetic scattering maximizes with $\mathbf{q}_1 = (\frac{1}{2}, 0, -\frac{1}{2})$ for $T < 213$ K, indicating that the magnetic ordering of Cu^{2+} is CM with the lattice structure. For $213 < T < 230$ K, momentum transfer $\mathbf{q}_2 \sim (0.507, 0, -0.486)$ and the magnetic ordering is incommensurate with the lattice structure.

Figure 2 shows scattering intensities with linearly polar-

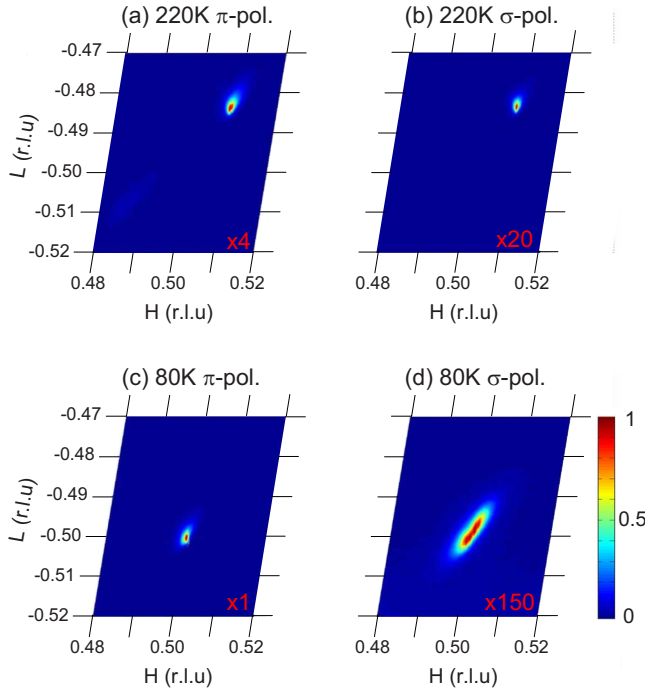


FIG. 3. (Color online) Two-dimensional distributions of magnetic scattering. (a) and (b) Intensity distributions in the a^*c^* plane from resonant soft x-ray magnetic scattering of CuO with π and σ polarizations at 220 K. (c) and (d) Distributions at 80 K.

ized x rays of π and σ polarizations at various temperatures as q changes in the direction oriented along the modulation vector \mathbf{Q} of the cycloidal spiral magnetic order, for which $\mathbf{Q} = \mathbf{q}_1 - \mathbf{q}_2$.¹² For π polarization, the magnetic scattering probes spins along the b axis and those in the ac plane. Temperature-dependent scattering data plotted in Figs. 2(a) and 2(c) show an ICM-CM transition at 213 K, consistent with previous neutron results.^{13,15} In addition, the incommensurate q shifts toward the CM modulation vector $(\frac{1}{2}, 0, -\frac{1}{2})$ as the temperature decreases from 230 K, implying that there exists a temperature-dependent competition of spin coupling between nearest and next-nearest neighbors in the $[10\bar{1}]$ chains. When the light polarization is switched to σ polarization, the measurement is sensitive to only spin components in the ac plane; the scattering intensity hence vanishes for magnetic ordering of pure collinear spin along the b axis. We found, however, that the magnetic scattering of σ polarization does not vanish in the CM collinear phase, leading to the following two scenarios. First, the finite measured intensity of magnetic scattering could result from any misalignment of the crystal orientation and the polarization of the incident x ray. Second, there exist ac components of spin in the CM phase of CuO. One can examine the former possibility through measuring the distributions of magnetic-scattering intensity in reciprocal space with incident x rays of π and σ polarizations. If the residual scattering intensity arises from a misalignment, the resonant magnetic scattering obtained with π and σ polarizations would have a similar distribution in the a^*c^* plane. As explained below, that first scenario is excluded.

For temperatures between T_{N1} and T_{N2} , e.g., 220 K, the

widths and intensities of scattering measured with these two polarizations are comparable, as shown in Figs. 3(a) and 3(b), consistent with neutron results indicating that CuO exhibits a spiral spin structure. In contrast, for temperatures below T_{N1} , the scattering distribution with σ polarization is markedly different from that of π polarization. For example, Fig. 3(d) shows that the scattering distribution of σ -polarized light at 80 K is anisotropic unlike that of π -polarized light shown in Fig. 3(c). Hence the finite measured scattering intensity with σ -polarized x rays does not result from misalignment.

The anisotropic scattering distribution with σ polarization is elongated along the modulation vector \mathbf{Q} of cycloidal spirals, leading us to suggest that there exist elongated magnetic domains oriented in a direction perpendicular to \mathbf{Q} and embedded in the collinear antiferromagnetic order. Seeking further numerical corroboration for the above hypothesis, we performed simulations of diffuse scattering using DISCUS software.²⁴ We first established a two-dimensional model crystal with short-range elongated domains of 2×2 reconstruction to mimic the magnetic ordering in the ac plane of CuO. Monte Carlo (MC) simulations were performed to minimize the energy of the model crystal comprising 500×500 unit cells with 10% 2×2 reconstruction. Second, we calculated diffuse scattering of the above model crystal using the Fourier transform in DISCUS according to the standard formula of kinematic scattering. Figure 4(a) shows a portion of the model crystal in real space obtained from MC simulations. Figure 4(b) plots the calculated scattering pattern

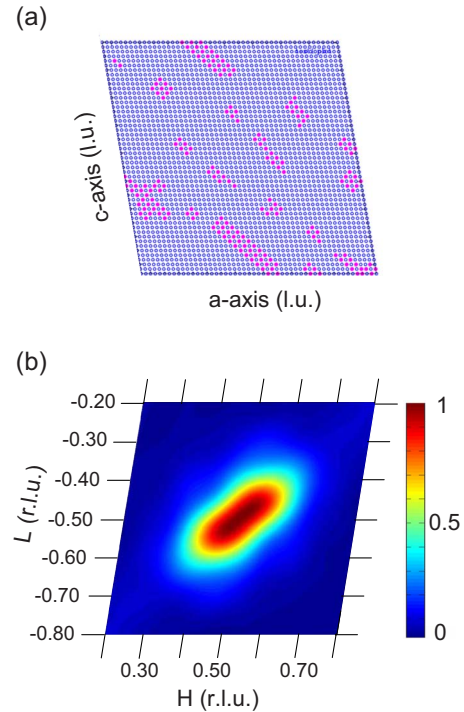


FIG. 4. (Color online) Simulations of diffuse scattering. (a) A portion (50×50 unit cells) of the model crystal with 2×2 reconstruction described in the text. Pink open circles are the 2×2 reconstruction domains to mimic the short-range magnetic order; blue circles denote the backbone lattice. (b) Calculated scattering pattern around $(\frac{1}{2}, -\frac{1}{2})$ in the a^*c^* plane corresponding to the model crystal.

around $(\frac{1}{2}, -\frac{1}{2})$ in reciprocal space. The simulations indicate that the diffuse scattering of elongated short-range 2×2 domain structures also yields an elongated pattern in reciprocal space, but in a perpendicular direction.

When combined with simulations of diffuse scattering, measurements of soft x-ray magnetic scattering lead us to propose a scenario for the underlying mechanism of the observed memory effect in the induced electric polarization. If we define the spin-correlation length as the inverse of the half width at half maximum of q scans, there exist elongated magnetic domains of size $\sim 180 \times 620 \text{ \AA}^2$ in the CM phase of CuO, and these magnetic nanoregions contain spins with finite components in the ac plane. Our another measurement (data are not shown here), i.e., linear dependence of magnetization on magnetic field through the origin, suggests no net canting moment. As the spiral nature of spins in the ICM phase, spin moments in these nanoregions are most likely spiral and form multiferroic nanoregions similar to polar

nanoregions observed in relaxor ferroelectrics.²⁵ However these nanoregions of spin spiral lead to no macroscopically measurable electric polarization, because of their nearly negligible volume fraction in comparison with that of collinear regions. Under warming of CuO across T_{N1} , the flip of spin handedness is energetically unfavorable²⁶ and the polarity of electric polarization remains unchanged. Hence there is exhibited a memory effect in the multiferroic transition through T_{N1} as a result of preserving the handedness of spin spirals in multiferroic nanoregions.

We thank S.-W. Cheong for discussions and NSRRC staff, particularly H. W. Fu and C. S. Lee, for their technical support. This work was supported in part by the National Science Council of Taiwan. Work at Osaka University was supported by KAKENHI (Grants No. 20674005 and No. 20001004) and Global COE Program, MEXT, Japan.

*Corresponding author; djhuang@nsrrc.org.tw

- ¹M. Imada, A. Fujimori, and Y. Tokura, *Rev. Mod. Phys.* **70**, 1039 (1998).
- ²N. A. Hill, *J. Phys. Chem. B* **104**, 6694 (2000).
- ³M. Fiebig, *J. Phys. D* **38**, R123 (2005).
- ⁴D. I. Khomskii, *J. Magn. Magn. Mater.* **306**, 1 (2006).
- ⁵W. Eerenstein, N. D. Mathur, and J. F. Scott, *Nature (London)* **442**, 759 (2006).
- ⁶S.-W. Cheong and M. V. Mostovoy, *Nat. Mater.* **6**, 13 (2007).
- ⁷T. Kimura, *Annu. Rev. Mater. Res.* **37**, 387 (2007).
- ⁸E. Dagotto, *Science* **309**, 257 (2005).
- ⁹L. E. Cross, *Ferroelectrics* **76**, 241 (1987).
- ¹⁰I. A. Sergienko and E. Dagotto, *Phys. Rev. B* **73**, 094434 (2006).
- ¹¹H. Katsura, N. Nagaosa, and A. V. Balatsky, *Phys. Rev. Lett.* **95**, 057205 (2005).
- ¹²T. Kimura, Y. Sekio, H. Nakamura, T. Siegrist, and A. Ramirez, *Nature Mater.* **7**, 291 (2008).
- ¹³T. Shimizu, T. Matsumoto, T. Goto, K. Yoshimura, and K. Kosuge, *J. Phys. Soc. Jpn.* **72**, 2165 (2003).
- ¹⁴B. X. Yang, T. R. Thurston, J. M. Tranquada, and G. Shirane, *Phys. Rev. B* **39**, 4343 (1989).
- ¹⁵J. B. Forsyth, P. J. Brown, and B. M. Wanklyn, *J. Phys. C* **21**, 2917 (1988).
- ¹⁶P. J. Brown, T. Chattopadhyay, J. B. Forsyth, V. Nunez, and F. Tasset, *J. Phys.: Condens. Matter* **3**, 4281 (1991).
- ¹⁷M. Ain, A. Menelle, B. M. Wanklyn, and E. F. Bertaut, *J. Phys.: Condens. Matter* **4**, 5327 (1992).
- ¹⁸C. Bucci and R. Fieschi, *Phys. Rev. Lett.* **12**, 16 (1964).
- ¹⁹D. Senff, P. Link, N. Aliouane, D. N. Argyriou, and M. Braden, *Phys. Rev. B* **77**, 174419 (2008).
- ²⁰A. H. Arkenbout, T. T. M. Palstra, T. Siegrist, and T. Kimura, *Phys. Rev. B* **74**, 184431 (2006).
- ²¹K. Taniguchi, N. Abe, S. Ohtani, and T. Arima, *Phys. Rev. Lett.* **102**, 147201 (2009).
- ²²See, for example, J. Okamoto, D. J. Huang, C.-Y. Mou, K. S. Chao, H.-J. Lin, S. Park, S.-W. Cheong, and C. T. Chen, *Phys. Rev. Lett.* **98**, 157202 (2007).
- ²³J. P. Hannon, G. T. Trammell, M. Blume, and D. Gibbs, *Phys. Rev. Lett.* **61**, 1245 (1988).
- ²⁴T. H. Proffen and R. B. Neder, *J. Appl. Crystallogr.* **30**, 171 (1997).
- ²⁵G. Xu, J. Wen, C. Stock, and P. M. Gehring, *Nature Mater.* **7**, 562 (2008).
- ²⁶Y. J. Choi, J. Okamoto, D. J. Huang, K. S. Chao, H. J. Lin, C. T. Chen, M. van Veenendaal, T. A. Kaplan, and S.-W. Cheong, *Phys. Rev. Lett.* **102**, 067601 (2009).